CHAPTER II

COMBINED FINITE ELEMENT AND MOMENT METHODS

This chapter describes the mathematical method applied in this thesis. The geometrical and equivalent network representations of the edge slot are presented as an introduction to the analysis of the edge slot. The formulation of the combined finite element and moment methods is begun by deriving the variational equation. Applying the method to solve this equation brings out the integrals that can be classified based on their domain to be integrals for cavity region, internal and external surfaces. These integrals are evaluated analytically, except the last integral that contains the external Green's function. The last is solved numerically by using Gauss quadrature integral approximation. This chapter also conducts the calculation of some characteristic parameters of the edge slot, such as admittance parameter, radiation pattern, etc.

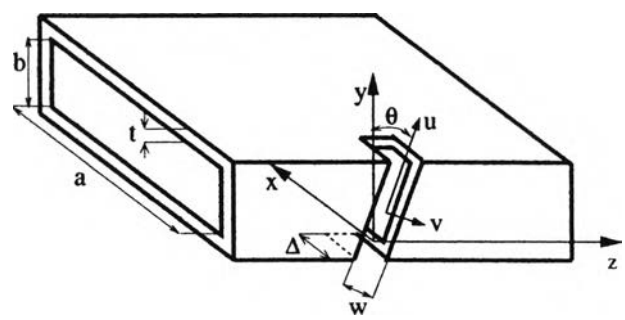

(a)

Figure 2.1: The coordinate system and geometrical parameters of the edge slot

2.1 Geometry of an Edge Slot

The geometry of the edge slot in which the analysis is confined is depicted in Fig. 2.1. An edge slot is cut in the narrow wall of the rectangular waveguide with tilting angle θ. The waveguide wall is assumed to be perfectly conducting, and has width a, height b and wall thickness t so that all modes except TE_{10} are cut off. This dominant mode is incident from the left end of the waveguide and a matched load follows the slot at the other end. The required resonant length of the slot is commonly more than the narrow wall height, thus the slot has extended parts, notated as Δ, on the top and bottom walls of the waveguide.

In case of finite wall thickness, the length of the slot along inner surface will be shorter than that of the outer surface. Consequently, the total slot length must be defined along the centerline of an edge slot. The length is determined as follows.

$$L = \frac{(b+t)}{\cos\theta} + 2\Delta - \frac{t}{2} \tag{2.1}$$

The next analysis also needs the unit vectors of the slot direction and slot width direction that are expressed as $\hat{u}$ and $\hat{v}$, respectively, depicted in Fig. (2.1). Since the slot is bent onto the top and bottom walls, its direction also varies as expressed below.

$$\begin{array}{ll} \bar{u} = -\hat{x} & \text{slot on the bottom wall} \\ \bar{u} = \hat{y}\cos\theta + \hat{z}\sin\theta & \text{slot on the side wall} \\ \bar{u} = \hat{x} & \text{slot on the top wall} \end{array} \tag{2.2}$$

Since the slot is cut inclinedly into the broad-wall, the metal surfaces, except those at the slot end, are not directed to $\hat{y}$ but are with inclination angle of θ. The direction of the slot width is perpendicular to this surface, thus it has similar direction for the whole parts of the slot.

$$\bar{v} = -\hat{y}\sin\theta + \hat{z}\cos\theta \tag{2.3}$$

2.2 Equivalent Network Representation of an Edge Slot

An edge slot cut on the rectangular waveguide causes some power emerged from the waveguide to the free-space. Thus, it can be modeled as a shunt obsta-

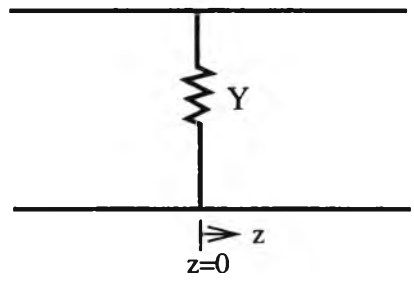

Figure 2.2: Transmission line equivalence of edge slot

cle on a two-wire transmission line, Fig.2.2. A transmission line of characteristic admittance G_0 is shunted at $z = 0$ by a lumped admittance Y [1],[17].

$$\frac{Y}{G_0} = \bar{g} + j\bar{b} \tag{2.4}$$

where g and b are the normalized conductance and susceptance of the slot.

These equivalent network parameters are related to the power distribution of the edge slot [17], as shown in the relation of impedance $\overline{Z}$:

$$\overline{Z} = \frac{P}{Z_0|\Delta I|^2} = \frac{P_r + j(P_j + Q_j)}{Z_0|\Delta I|^2} = \frac{1}{\bar{g} + j\bar{b}} \tag{2.5}$$

where P is the total reactive power of equivalent magnetic current of slot, P_r is the portion of P radiated into the free space, P_j and Q_j are portions of P stored, respectively, outside and inside the waveguide around the slot, ΔI is the discontinuity in modal current, and Z_0 is the wave impedance of the excitation mode in the waveguide. The slot is said to be resonant if Y/G_0 is pure real.

The value of the admittance can be calculated with a simple relation between the normalized admittance and reflection coefficient Γ that given as [17].

$$\frac{Y}{G_0} = -\frac{2\Gamma}{1+\Gamma} \tag{2.6}$$

The reflection coefficient can be related to the field in the slot by:

$$\Gamma = \frac{(\pi/a)^2}{\omega\mu_0\beta_{inc}ab} \int_{slot} \overline{E}_s \times \overline{H}_{inc} \cdot \bar{n}\, ds \tag{2.7}$$

with $\bar{n}$ is the unit vector on the internal boundary surface inward the waveguide.

Using the above relations, once we know the electric field distribution along the slot, the network parameter can be calculated. The resonant length of the slot also can be determined by taking the zero crossing of susceptance graph.

It is worth noting that the resonant conductance and the resonant length are important parameters in the design of slotted waveguide array. Therefore, it is desirable to be able to predict these parameters accurately.

2.3 Formulation of Combined Finite Element and Moment Method

The moment method generally provides efficient and accurate means of analyzing the scattering and radiation properties of the slot waveguide antenna. However, the conventional moment method is not suitable for the analysis of the edge slot when accounting for the wall thickness. Since the required analytical expression of the dyadic Green's function for the cavity region caused by the wall thickness is unavailable. This Green's function is difficult to formulate due to the complexity of the slot structure.

The moment method must couple with other method to circumvent this problem. One of the methods that can be used is the finite element method. Initially, an equivalence principle is invoked to divide the problem domain into separate regions, which are then coupled by enforcing the continuity condition at the interfaces of these regions. The fields on the boundary surfaces are expressed by appropriate Green's functions as done by the conventional moment method. While the field inside the slot aperture is formulated in terms of a functional which is a feature of the finite element method. Therefore, it is unnecessary to have a prior knowledge of the dyadic Green's function of the slot-cavity region.

2.3.1 Field Equivalent Principle

Using the field equivalence principle [18], it can be assumed that the slot is closed by a perfect electric conductor. To ensure the continuity of tangential electric fields at the slot location, a set of magnetic current sheets is placed at the

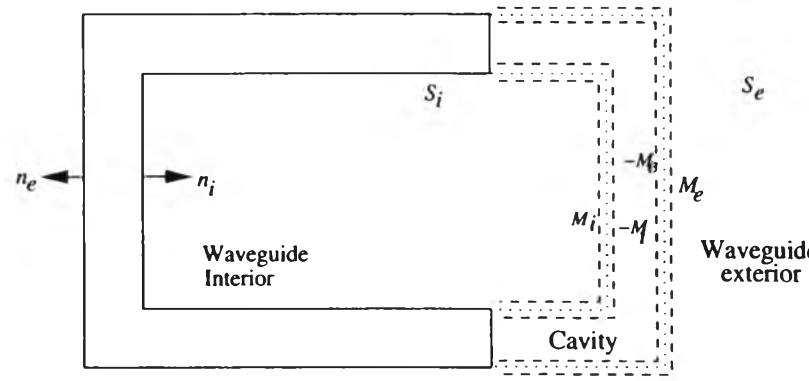

Figure 2.3: The field equivalence on the edge slot

slot apertures, as shown in Fig. 2.3. This procedure decouples the original domain of the problem into three separate regions, namely

- the region interior to the waveguide
- the region exterior to the waveguide
- the cavity region formed due to the waveguide wall thickness

In the interior region, the electromagnetic field is the sum of the incident and the field produced by the surface magnetic current $\overline{M}_i$. In the cavity region, the electromagnetic field is the field produced by the surface magnetic currents $\overline{M}_i$ and $\overline{M}_e$. Similarly, the field in the exterior region is the field generated by the magnetic current $\overline{M}_e$.

By applying continuity conditions for tangential component of the magnetic field on the surface S_i and S_e, we can obtain:

$$\bar{n}_i \times \overline{H}_{inc}(\bar{r}) + \bar{n}_i \times \overline{H}_{int}(\bar{r}) = \bar{n}_i \times \overline{H}_{cav}(\bar{r}) \qquad on \;\; S_i \tag{2.8}$$

$$\bar{n}_e \times \overline{H}_{cav}(\bar{r}) - \bar{n}_e \times \overline{H}_{ext}(\bar{r}) = 0 \qquad on \;\; S_e \tag{2.9}$$

Next, a dyadic Green's function of magnetic type is introduced [19], which satisfies the following equation

$$\nabla \times \nabla \overline{\overline{G}}(\bar{r}, \bar{r}') - k^2 \overline{\overline{G}}(\bar{r}, \bar{r}') = -\overline{\overline{I}}\delta(\bar{r} - \bar{r}') \tag{2.10}$$

$$\bar{n} \times \nabla \times \overline{\overline{G}}(\bar{r}, \bar{r}') = 0 \tag{2.11}$$

with $\overline{\overline{I}} = \hat{x}\hat{x} + \hat{y}\hat{y} + \hat{z}\hat{z}$ and k is the wave number. Using the Green's function, it is possible to calculate the magnetic field of each region.

$$\overline{H}(\bar{r}) = j\omega\epsilon \oint \overline{\overline{G}}(\bar{r},\bar{r}') \cdot \overline{M}(\bar{r}')ds' \tag{2.12}$$

where ω is the angular frequency, ϵ is the permittivity. The surface integral is taken over the source region r' in the problem domain. If the magnetic fields in the three regions are represented by (2.12) and the resultant expressions are substituted into (2.8) and (2.9) the following integral equations are formed

$$\begin{aligned} j\omega\epsilon\bar{n}_i \times & \iint_s \left[\overline{\overline{G}}_{cav}(\bar{r},\bar{r}') - \overline{\overline{G}}_{int}(\bar{r},\bar{r}')\right] \cdot M_i(\bar{r}')ds' \\ + & \; j\omega\epsilon\bar{n}_i \times \iint_s \overline{\overline{G}}_{cav}(\bar{r},\bar{r}') \cdot M_e(\bar{r}')ds' = \bar{n}_i \times H^{inc}(\bar{r}) \end{aligned} \tag{2.13}$$

$$\begin{aligned} j\omega\epsilon\bar{n}_e \times & \iint_s \overline{\overline{G}}_{cav}(\bar{r},\bar{r}') \cdot M_i(\bar{r}')ds' \\ + & \; j\omega\epsilon\bar{n}_e \times \iint_s \left[\overline{\overline{G}}_{cav}(\bar{r},\bar{r}') - \overline{\overline{G}}_{ext}(\bar{r},\bar{r}')\right] \cdot M_e(\bar{r}')ds' = 0 \end{aligned} \tag{2.14}$$

where $\overline{\overline{G}}_{int,ext,cav}$ denotes the dyadic Green's function in the interior, exterior and cavity region. The equivalent magnetic current $\overline{M}_s$ can be formulated as a function of the electric field $\overline{E}$ with the relation:

$$\overline{M}_s = \overline{E} \times \bar{n} \tag{2.15}$$

The electric field distribution along the slot can be calculated by solving those integral equations. Unfortunately, the Green's function of the cavity region has not been exactly formulated yet. It is the reason of ignorance of the wall thickness in some researches. This formulation is also partly used in other investigations either in the finite element method.

2.3.2 Reaction Variational Equation

The formulation of the finite element method is taken from the variational equation derived in [17]. It is derived from the variational reaction theory adopted from [20].

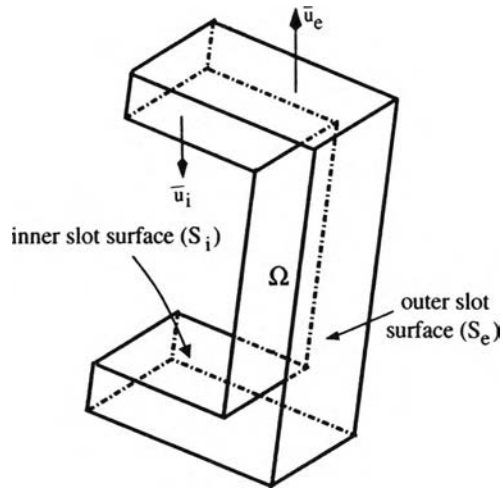

Figure 2.4: The domain of the problem

The derivation of the variational equation is commenced from the reaction:

$$\delta\psi = \iiint_{\Omega} (\delta\overline{E} \cdot \overline{J}) d\Omega = 0 \tag{2.16}$$

where $\overline{E}$ is the trial function and $\overline{J}$ is the trial source supporting the trial field with the relation:

$$\overline{J} = \nabla \times \overline{H} - j\omega\epsilon_0\overline{E} \tag{2.17}$$

Substituting (2.17) into(2.16), and employing the divergence theorem of Gauss, the reaction form becomes:

$$\begin{aligned} \delta\Psi &= \iiint_{\Omega} (\delta\overline{E} \cdot \nabla \times \overline{H} - j\omega\epsilon_0\delta\overline{E} \cdot \overline{E}) d\Omega \\ &= \iint_{S_i} (\bar{n}_i \cdot \overline{H} \times \delta\overline{E}) ds + \iint_{S_e} (\bar{n}_e \cdot \overline{H} \times \delta\overline{E}) ds \\ &+ \iiint_{S_i} (\overline{H} \cdot \nabla \times \delta\overline{E} - j\omega\epsilon_0\delta\overline{E} \cdot \overline{E}) d\Omega \end{aligned} \tag{2.18}$$

where $\bar{n}_i$ and $\bar{n}_e$ denote the unit vector outward normal to slot surface S_i and S_e, respectively. It can be seen that the domain of problems consists of the cavity region and the surface area of S_i and S_e as shown in figure 2.4.

The magnetic field $\overline{H}$ is brought into the term of trial electric field by invoking the formulation of the magnetic field in the inner surface and outer surface as expressed in equation (2.13) and (2.14) and the magnetic field inside the cavity

region:

$$\overline{H} = -\frac{1}{j\omega\mu_0}\nabla \times \overline{E} \tag{2.19}$$

After the substitution, the following variational equation is obtained.

$$\begin{aligned}
\partial\Psi' &= 0 \\
\Psi' &= -\frac{\Psi}{j\omega\epsilon_0} \\
&= \frac{1}{2}\iiint_{\Omega}\left(\overline{E}\cdot\overline{E} - \frac{1}{k^2}\nabla\times\overline{E}\cdot\nabla\times\overline{E}\right)d\Omega \\
&\quad +\frac{1}{2}\iint_{S_i}\iint_{S_i}\bar{n}_i\times\overline{E}(\bar{r})\cdot\overline{\overline{G}}_{int}(\bar{r},\bar{r}')\cdot\bar{n}_i\times\overline{E}(\bar{r})ds'ds \\
&\quad +\frac{1}{2}\iint_{S_e}\iint_{S_e}\bar{n}_e\times\overline{E}(\bar{r})\cdot\overline{\overline{G}}_{ext}(\bar{r},\bar{r}')\cdot\bar{n}_e\times\overline{E}(\bar{r})ds'ds \\
&\quad +\frac{1}{j\omega\epsilon_0}\iint_{S_i}\overline{H}^{inc}\cdot\bar{n}_i\times\overline{E}(\bar{r})ds
\end{aligned} \tag{2.20}$$

This variational equation has been proved in [11] to be stationary at the exact solution of the unknown electric field. The problem in the above equation can be classified in terms of cavity region Ω, internal and external boundary surfaces (S_i and S_e).

The field is simplified by assuming the narrow slot case that the electric field is constant across the slot width. It is expressed by:

$$\overline{E}(\bar{r}) = \bar{v}E_v(\bar{r}) = \bar{v}\phi(\bar{r}) \tag{2.21}$$

While the vector of slot width direction ($\bar{v}$) is shown in (2.3). Substituting (2.21) into (2.20), the variational equation becomes a simpler form in terms of the scalar unknown $\phi(\overline{R})$.

$$\begin{aligned}
\Psi' &= \frac{1}{2}\iiint_{\Omega}\left(\phi^2 - \frac{1}{k^2}\left[\nabla\phi\cdot\nabla\phi - (\bar{v}\cdot\phi)^2\right]\right)d\Omega \\
&\quad +\frac{1}{2}\iint_{S_i}\iint_{S_i}\phi(\bar{r})\cos\alpha\;\bar{u}\cdot\overline{\overline{G}}_{int}(\bar{r},\bar{r}')\cdot\bar{u}'\;\phi(\bar{r})\cos\alpha'\;ds'ds \\
&\quad +\frac{1}{2}\iint_{S_e}\iint_{S_e}\phi(\bar{r})\cos\alpha\;\bar{u}\cdot\overline{\overline{G}}_{ext}(\bar{r},\bar{r}')\cdot\bar{u}'\;\phi(\bar{r})\cos\alpha'\;ds'ds \\
&\quad +\frac{1}{j\omega\epsilon_0}\iint_{S_i}\overline{H}^{inc}\cdot\bar{u}\phi(\bar{r})\cos\alpha\;ds
\end{aligned} \tag{2.22}$$

where

$$\alpha = \begin{cases} \theta, & \bar{r} \text{ on the broad-wall} \\ 0, & \bar{r} \text{ on the narrow-wall} \end{cases} \tag{2.23}$$

The unknown electric field distribution ϕ in the above variational equation can be solved with finite element method which is coupled with moment method to calculate the field in the boundary surface S_i and S_e. The explanation of this method is separated in terms of field inside the cavity which is denoted by the first integration and the field on both boundary surfaces.

2.3.3 The formulation of fields in cavity region

The cavity region that exists due to the finite wall thickness is occupied by six surfaces on its boundary. Four surfaces are the waveguide wall in which the slot is cut. The inner and outer surfaces are the prefect electric conductor sheet taken from the assumption of field equivalence principle.

A part of the formulation regarding the fields in the cavity region is expressed in the first integral of RHS of (2.20). Based on the assumption of the narrow slot case, the unknown field ϕ is constant across the width of the slot. Therefore, the volume integral can be simplified into surface integral as follows:

$$\begin{aligned} &\iiint_{\Omega} \phi^2 - \frac{1}{k^2}\left[\nabla\phi\cdot\nabla\phi - (\hat{v}\cdot\nabla\phi)^2\right] d\Omega \\ &\quad = w\iint_{A_\Omega} \phi^2 - \frac{1}{k^2}\left[\nabla\phi\cdot\nabla\phi - (\hat{v}\cdot\nabla\phi)^2\right] dA_\Omega \\ &\quad = w\iint_{A_\Omega} \phi^2 dA_\Omega - \frac{w}{k^2}\iint_{A_\Omega} \nabla\phi\cdot\nabla\phi dA_\Omega + \frac{w}{k^2}\iint_{A_\Omega} (\hat{v}\cdot\nabla\phi)^2 dA_\Omega \end{aligned} \tag{2.24}$$

where w is the width of the slot and A_Ω is the area of side surfaces of the Ω region.

These fields are calculated by the finite element method with the procedure consisting of the following basic steps [21]:

- Discretization or subdivision of the domain
- Selection of the interpolation functions
- Formulation of the system of equations

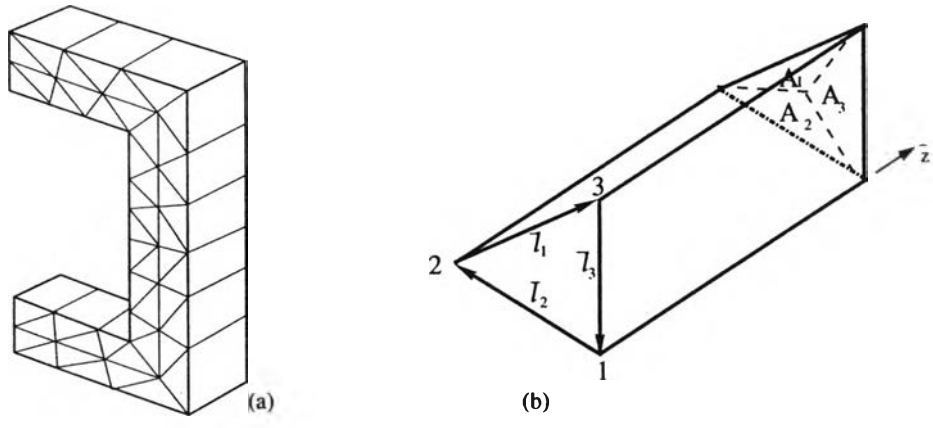

Figure 2.5: The domain is divided into elements

- Solution of the system equations

The first step, the domain is divided into n layers, with each layer divided into $2N$ small triangular cylinder, as shown in the Fig. 2.5. Hence, the total number of elements $N = 2N^b + N^n$, which N^b and N^n represent the number of elements in the broad wall and narrow wall, respectively. After discretization, we get the formulation in terms of small element.

$$\iiint_{\Omega} \phi^2 - \frac{1}{k^2}\left[\nabla\phi \cdot \nabla\phi - (\hat{v} \cdot \nabla\phi)^2\right] d\Omega = \sum_e \left[\sum_{i=1}^{3}\sum_{j=1}^{3} G_{ij}^{(e)}\right]$$

where

$$G_{ij}^{(e)} = \left(w \iint_{A^e} \phi_i\phi_j dA^e - \frac{w}{k^2}\iint_{A^e} \nabla\phi_i \cdot \nabla\phi_j dA^e + \frac{w}{k^2}\iint_{A^e} (\hat{v} \cdot \nabla\phi_i)(\hat{v} \cdot \nabla\phi_j) dA^e\right) \tag{2.25}$$

The second step, a standard interpolation based on triangular area coordinate is chosen. The unknown of the electric field is expanded as:

$$\phi(\bar{r}) = \sum_{i=1}^{3} \phi_i^{(e)} L_i(\bar{r}) \tag{2.26}$$

where $\phi_i^{(e)}$'s are the unknown fields at the nodes 1,2, and 3 of the e-th element. The coefficient L_i is the shape function of node i that is defined by

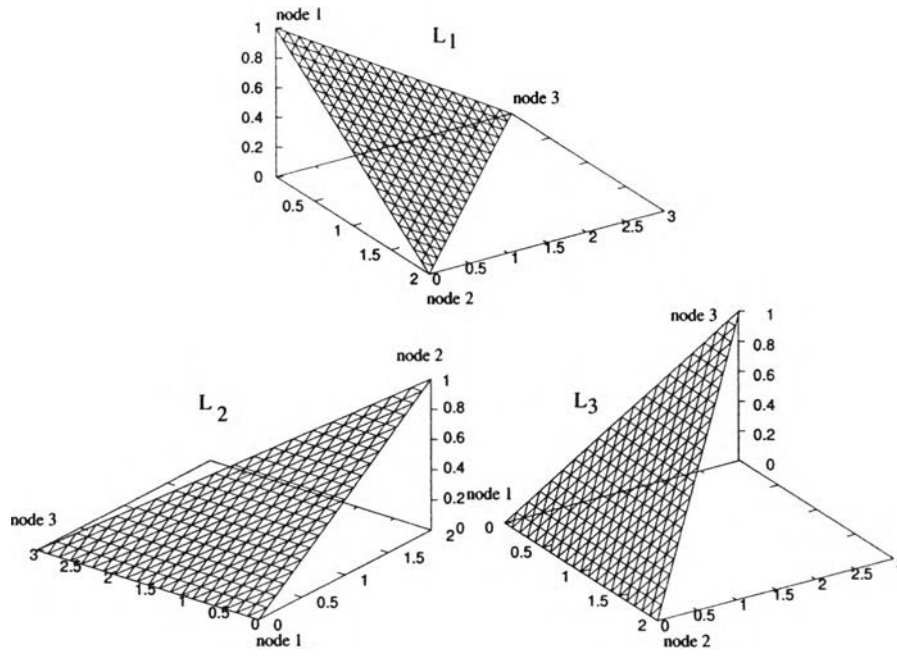

Figure 2.6: The linear characteristic of the area coordinate shape function

$$L_i = \frac{1}{2A_e}(a_i + b_i x + c_i y) \qquad i = 1, 2, 3 \tag{2.27}$$

in which

$$\begin{array}{lll} a_1 = x_2y_3 - x_3y_2 & a_2 = x_3y_1 - x_1y_3 & a_3 = x_1y_2 - x_2y_1 \\ b_1 = y_2 - y_3 & b_2 = y_3 - y_1 & b_3 = y_1 - y_2 \\ c_1 = x_3 - x_2 & c_2 = x_1 - x_3 & c_3 = x_2 - x_1 \end{array} \tag{2.28}$$

and A_e is the area of element given by

$$A^e = \frac{1}{2}\begin{bmatrix} 1 & x_1 & y_1 \\ 1 & x_2 & y_2 \\ 1 & x_3 & y_3 \end{bmatrix} = \frac{1}{2}(b_1c_2 - b_2c_1) \tag{2.29}$$

It is worth noting that this shape function has linear characteristic as depicted in Fig. 2.6

The third step is substituting the expanding function to (2.25). It is analyzed separately for each integral. The first integral can be evaluated analytically by using the basic formula for triangle area integration

$$\iint_{A_e} (L_1^e)^l (L_2^e)^m (L_3^e)^n dxdy = \frac{l!m!n!}{(l+m+n+2)!} 2A_e \tag{2.30}$$

resulting in

$$w\iint_{A_e}\phi_i\phi_j dA_e = w\iint_{A_e}L_i(\bar{r})L_j(\bar{r})dA_e = \begin{cases}\frac{V^{(e)}}{6} & i=j\\ \frac{V^{(e)}}{12} & i\neq j\end{cases} \tag{2.31}$$

where $V^{(e)} = A^{(e)}$ is the volume of the e-th element.

The second integral is evaluated using the relations

$$\begin{aligned}\nabla L_i &= \frac{\partial L_i}{\partial x}\hat{a}_x + \frac{\partial L_i}{\partial y}\hat{a}_y\\ \frac{\partial L_i}{\partial x} &= \frac{\partial}{\partial x}\left(\frac{1}{2A_e}(a_i + b_i x + c_i y)\right) = \frac{1}{2A_e}b_i\\ \frac{\partial L_i}{\partial y} &= \frac{\partial}{\partial y}\left(\frac{1}{2A_e}(a_i + b_i x + c_i y)\right) = \frac{1}{2A_e}c_i\end{aligned}$$

thus it yields

$$\frac{w}{k^2}\iint_{A_e}\nabla\phi\cdot\nabla\phi dA_e = \frac{w}{k^2}\iint_{A_e}\nabla L_i\cdot\nabla L_j dA_e = \frac{w}{k^2}\left(\frac{b_i b_j + c_i c_j}{4A_e}\right) \tag{2.32}$$

The last integral is equal to zero since the vector $\bar{v}$ is always perpendicular to the area A_e thus $\bar{v}\cdot\nabla L_i = 0$.

Now, we get the expression of the integral for the cavity region as expressed in (2.30) and (2.32) that can be calculated with simple programming. The value of each element from the integration is arranged in the matrix, simply notated as matrix G.

2.3.4 The formulation of fields on the inner surfaces

The fields on the inner surfaces of the slot consist of the incident field from the waveguide and the field due to the magnetic current density on the surface. They are expressed by the second and fourth integrals of right hand side of equation (2.22). For simplification, these integrals are called as incident wave and magnetic current integral, respectively. These equations are basically derived from the magnetic field integral equation for the inner surface as mentioned in (2.13). The nature of the finite element is not suitable for solving the integral equation, thus it must be combined with the moment method to evaluate it. The segmentation and basis function of the moment method must be compatible with the finite element method

for the cavity region. The characteristic of area coordinate shape function used in the cavity region is linear. Thus, it becomes triangular basis function on the surface integrals.

Initially, the surface is discretized into surface elements following the meshing of the cavity and expanding the unknown ϕ into basis function. To ease the program development, it is expressed as follows.

$$\phi(\bar{n}) = \sum_{i=1}^{2} N_i \phi_i \tag{2.33}$$

with

$$\begin{aligned} N_1(u) &= \frac{u_2 - u}{u_2 - u_1} \\ N_2(u) &= \frac{u - u_1}{u_2 - u_1} \end{aligned} \tag{2.34}$$

where $u_{1,2}$ is the coordinate of node points to the slot directions.

Substituting (2.33) into the integrals, we get

$$\frac{1}{j\omega\epsilon_0} \iint_{S_i} \overline{H}_u^{inc} \phi(\bar{r}) \cos\alpha \, ds = \sum_{e=1}^{N} \sum_{i=1}^{2} H_i^{(e_{int})} \phi_i^{(e_{int})} \tag{2.35}$$

$$\begin{aligned} \frac{1}{2} \iint_{S_i} \iint_{S_i} & \phi(\bar{r}) \cos\alpha \, \hat{u}_i \cdot \overline{\overline{G}}_{int}(\bar{r}, \bar{r}') \cdot \hat{u}_i' \, \phi(\bar{r}) \cos\alpha' ds' ds \\ &= \frac{1}{2} \sum_{e_{int}=1}^{N} \sum_{e'_{int}=1}^{N} \left[\sum_{i=1}^{2} \phi_i^{(e_{int})} Y_{ij}^{(e_{int})} \phi_j^{(e_{int})} \right] \end{aligned} \tag{2.36}$$

where

$$H_i^{(e_{int})} = \frac{1}{j\omega\epsilon_0} \iint_{S_i} H_u^{inc} N_i(u) \cos\alpha \, ds \tag{2.37}$$

$$Y_{ij}^{(e_{int})} = \iint_{S_i} \iint_{S_i} N_i(u) \cos\alpha \, \hat{u} \cdot \overline{\overline{G}}_{int}(\bar{r}, \bar{r}') \cdot \hat{u}' \, N_i(u') \cos\alpha' \, ds' ds \tag{2.38}$$

The notation of e_{int} denotes the element on the internal surfaces. Equation (2.38) may be interpreted as the $\bar{u}$ directed magnetic field on the element e_{int} due to all magnetic current source in the element e'_{int}. The parameters related with the source are signed with prime notation.

2.3.4.1 Integral of incident wave

The incident wave is dominant mode TE_{10} that its magnetic field can be expressed as follow with the coordinate system is shown in Fig. 2.1.

$$\begin{aligned} H_x &= H_0 \sin\left(\frac{\pi x}{a}\right) e^{-k_{10}z} \\ H_y &= 0 \\ H_z &= \frac{\pi}{k_{10}a} H_0 \cos\left(\frac{\pi x}{a}\right) e^{-k_{10}z} \end{aligned} \tag{2.39}$$

where H_0 denotes the amplitude of the incident wave which is normalized to unity, a is the width of the waveguide and k_{10} is the wave impedance of the dominant mode in the waveguide

$$k_{10} = \sqrt{\left(\frac{\pi}{a}\right)^2 - k^2}$$

where k is the free space wave number.

The direction of the slot is varied along the slot, as shown by the vector in (2.100). Thus, the coefficient H_u^{inc} in (2.37) can be divided in terms of the slot parts.

$$\begin{aligned} H_u^{inc} &= \overline{H}^{inc} \cdot \bar{u}_{bottom} &&= -H_x && \text{on the bottom part} \\ H_u^{inc} &= \overline{H}^{inc} \cdot \bar{u}_{side} &&= H_z \sin\theta && \text{on the side part} \\ H_u^{inc} &= \overline{H}^{inc} \cdot \bar{u}_{top} &&= H_x && \text{on the top part} \end{aligned} \tag{2.40}$$

Using the expressions (2.40), the integral of the incident wave (2.37) can be evaluated in each slot part.

The slot on the top wall has direction $\hat{u} = \hat{x}$. Thus, H_i^{inc} in (2.37) can be expressed as

$$H_i^{(e_{int})} = \frac{1}{j\omega\epsilon_0} \iint_{S_i} H_x N_i(u) \cos\alpha \, ds \tag{2.41}$$

$$= \frac{1}{j\omega\epsilon_0} \iint_{S_i} \sin(k_x x) e^{-k_{10}z} N_i(x) \cos\alpha \, ds \tag{2.42}$$

To get more detail derivation, the integral is evaluated for N_1 and N_2

$$H_1^{(e_{int})} = \frac{\cos\theta}{j\omega\epsilon_0} \int_{x_1}^{x_2} \int_{z_1}^{z_1+w} \sin(k_x x) e^{-k_{10}z} \frac{(x - x_1)}{(x_2 - x_1)} \, dz \, dx \tag{2.43}$$

$$H_2^{(e_{int})} = \frac{\cos\theta}{j\omega\epsilon_0} \int_{x_1}^{x_2} \int_{z_1}^{z_1+w} \sin(k_x x) e^{-k_{10}z} \frac{(x_2 - x)}{(x_2 - x_1)} \, dz \, dx \tag{2.44}$$

The coefficients $x_{1,2}$ are the coordinate of two successive nodes in the inner surface and w is the slot width.

Initially, the first integration over the z axis is evaluated

$$H_1^{(e_{int})} = \frac{\cos\theta}{j\omega\epsilon_0}\int_{x_1}^{x_2}\sin(k_x x)\frac{(x-x_1)}{(x_2-x_1)}\left[-\frac{e^{-k_{10}z}}{k_{10}}\right]_{z_i}^{z_i+w}dx$$
$$= \frac{\cos\theta}{j\omega\epsilon_0}\frac{(1-e^{-k_{10}w})}{k_{10}}e^{-k_{10}z}\int_{x_1}^{x_2}\sin(k_x x)\frac{(x-x_1)}{(x_2-x_1)}dx \quad (2.45)$$

$$H_2^{(e_{int})} = \frac{\cos\theta}{j\omega\epsilon_0}\int_{x_1}^{x_2}\sin(k_x x)\frac{(x_2-x)}{(x_2-x_1)}\left[-\frac{e^{-k_{10}z}}{k_{10}}\right]_{z_i}^{z_i+w}dx$$
$$= \frac{\cos\theta}{j\omega\epsilon_0}\frac{(1-e^{-k_{10}w})}{k_{10}}e^{-k_{10}z}\int_{x_1}^{x_2}\sin(k_x x)\frac{(x_2-x)}{(x_2-x_1)}dx \quad (2.46)$$

Next, the integration over the x axis is solved by the partial integration and we get

$$H_1^{(e_{int})} = \frac{\cos\theta}{j\omega\epsilon_0}\frac{(1-e^{-k_{10}w})}{k_{10}}e^{-k_{10}z}$$
$$\cdot\left[-\frac{(x-x_1)}{(x_2-x_1)}\frac{\cos(k_x x)}{k_x}+\frac{1}{(x_2-x_1)}\frac{\sin(k_x x)}{k_x^2}\right]_{x_1}^{x_2} \quad (2.47)$$

$$H_2^{(e_{int})} = \frac{\cos\theta}{j\omega\epsilon_0}\frac{(1-e^{-k_{10}w})}{k_{10}}e^{-k_{10}z}$$
$$\cdot\left[-\frac{(x_2-x)}{(x_2-x_1)}\frac{\cos(k_x x)}{k_x}-\frac{1}{(x_2-x_1)}\frac{\sin(k_x x)}{k_x^2}\right]_{x_1}^{x_2} \quad (2.48)$$

The portion of the slot on the bottom wall has direction $\hat{u}=-\hat{x}$, thus it can be evaluated in the similar way to the top slot. It is noted that $x_i < x_{i-1}$ and $x_i > x_{i+1}$, so we get

$$H_i^{(e_{int})} = -\frac{\cos\theta}{j\omega\epsilon_0}\frac{(1-e^{-k_{10}w})}{k_{10}}e^{-k_{10}z}$$
$$\cdot\left[-\frac{(x-x_1)}{(x_2-x_1)}\frac{\cos(k_x x)}{k_x}+\frac{1}{(x_2-x_1)}\frac{\sin(k_x x)}{k_x^2}\right]_{x_2}^{x_1} \quad (2.49)$$

$$H_i^{(e_{int})} = -\frac{\cos\theta}{j\omega\epsilon_0}\frac{(1-e^{-k_{10}w})}{k_{10}}e^{-k_{10}z}$$
$$\cdot\left[-\frac{(x_2-x)}{(x_2-x_1)}\frac{\cos(k_x x)}{k_x}-\frac{1}{(x_2-x_1)}\frac{\sin(k_x x)}{k_x^2}\right]_{x_2}^{x_1} \quad (2.50)$$

The direction of the slot on the side wall is inclined with θ angle, $\hat{u}=\hat{y}\cos\theta+$

$\hat{z}\sin\theta$, so the expression of the incident wave integration can be written as

$$H_i^{(e_{int})} = \frac{1}{j\omega\epsilon_0}\iint_{S_i} H_z \sin\theta N_i(u)\cos\alpha \, ds \tag{2.51}$$

$$= \frac{1}{j\omega\epsilon_0}\iint_{S_i} \frac{\pi\sin\theta}{k_{10}a}\cos(k_x x)e^{-k_{10}z}N_i(u)\, ds \tag{2.52}$$

Taking analogous to the step on the broad wall, the first integral over the z axis is firstly solved and we get

$$H_i^{(e_{int})} = \frac{1}{j\omega\epsilon_0}\frac{(1-e^{-k_{10}w})}{k_{10}}\int_{u_1}^{u_2}\frac{\pi\sin\theta}{k_{10}a}\cos(k_x x)e^{-k_{10}z}N_i(u)\, du \tag{2.53}$$

Based on the needs on the programming, it is derived for each N_i's.

$$H_1^{(e_{int})} = \frac{1}{j\omega\epsilon_0}\frac{(1-e^{-k_{10}w})}{k_{10}}\frac{\pi\sin\theta}{k_{10}a}\cos(k_x x)\int_{u_1}^{u_2} e^{-k_{10}z}\frac{(u_2-u)}{(u_2-u_1)}\, du \tag{2.54}$$

$$H_2^{(e_{int})} = \frac{1}{j\omega\epsilon_0}\frac{(1-e^{-k_{10}w})}{k_{10}}\frac{\pi\sin\theta}{k_{10}a}\cos(k_x x)\int_{u_1}^{u_2} e^{-k_{10}z}\frac{(u-u_1)}{(u_2-u_1)}\, du \tag{2.55}$$

Remembering that $z = u\sin\theta$ the integrals on $H_1^{(e_{int})}$ and $H_2^{(e_{int})}$ can be evaluated using the formulae of partial integration. So we get the final form of both integrals as follows

$$\begin{aligned} H_2^{(e_{int})} &= \frac{1}{j\omega\epsilon_0}\frac{(1-e^{-k_{10}w})}{k_{10}}\frac{\pi\sin\theta}{k_{10}a}\cos(k_x x)\int_{u_1}^{u_2} e^{-k_{10}u\sin\theta}\frac{(u_2-u)}{(u_2-u_1)}\, du \\ &= \frac{1}{j\omega\epsilon_0}\frac{(1-e^{-k_{10}w})}{k_{10}}\frac{\pi\sin\theta}{k_{10}a}\cos(k_x x) \\ &\quad\cdot\left[-\frac{(u_2-u)}{(u_2-u_1)}\frac{e^{-k_{10}u\sin\theta}}{k_{10}\sin\theta}+\frac{1}{(u_2-u_1)}\frac{e^{-k_{10}u\sin\theta}}{(k_{10}\sin\theta)^2}\right]_{u_1}^{u_2} \end{aligned} \tag{2.56}$$

$$\begin{aligned} H_1^{(e_{int})} &= \frac{1}{j\omega\epsilon_0}\frac{(1-e^{-k_{10}w})}{k_{10}}\frac{\pi\sin\theta}{k_{10}a}\cos(k_x x)\int_{u_1}^{u_2} e^{-k_{10}u\sin\theta}\frac{(u-u_1)}{(u_2-u_1)}\, du \\ &= \frac{1}{j\omega\epsilon_0}\frac{(1-e^{-k_{10}w})}{k_{10}}\frac{\pi\sin\theta}{k_{10}a}\cos(k_x x) \\ &\quad\cdot\left[-\frac{(u-u_1)}{(u_2-u_1)}\frac{e^{-k_{10}u\sin\theta}}{k_{10}\sin\theta}-\frac{1}{(u_2-u_1)}\frac{e^{-k_{10}u\sin\theta}}{(k_{10}\sin\theta)^2}\right]_{u_1}^{u_2} \end{aligned} \tag{2.57}$$

2.3.4.2 Internal Green's function and its integral

The internal Green's function is natural to use the waveguide dyadic Green's function which is formulated as follows

$$\begin{aligned}\overline{\overline{G}}_{int}(\overline{r},\overline{r}') &= \sum_{m=0}^{\infty}\sum_{n=0}^{\infty}\frac{\epsilon_m\epsilon_n}{2abk_{mn}}\left(\overline{\overline{I}}+\frac{\nabla\nabla}{k^2}\right)e^{-k_{mn}|z-z'|} \\ &\quad\cdot\left[\hat{x}\hat{x}\;S_xS_x'C_yC_y'+\hat{y}\hat{y}\;C_xC_x'S_yS_y'+\hat{z}\hat{z}\;C_xC_x'C_yC_y'\right] \\ &\quad (m,n)\neq(0,0)or(1,0) \end{aligned} \tag{2.58}$$

$$\begin{array}{ll} k_x=\frac{m\pi}{a} & k_y=\frac{n\pi}{b} \\ k_{mn}=[k_x^2+(k_y)^2-k^2]^{1/2} & k=\frac{2\pi}{\lambda} \\ C_x=\cos k_xx & C_x'=\cos k_xx' \\ S_x=\sin k_xx & S_x'=\sin k_xx' \\ C_y=\cos k_yy & C_y'=\cos k_yy' \\ S_y=\sin k_yy & S_y'=\sin k_yy' \end{array} \tag{2.59}$$

where $\overline{\overline{I}}=\hat{x}\hat{x}+\hat{y}\hat{y}+\hat{z}\hat{z}$ is the unit tensor, a and b are the waveguide dimensions and ϵ_m is the Neumann factor such that $\epsilon_m=1$ if $m=0$ and $\epsilon_m=2$ if $m\neq 0$. To simplify the expression, it can be presented in the matrix form as follows

$$\overline{\overline{G}}_{int}=\begin{bmatrix} G_{xx} & 0 & 0 \\ 0 & G_{yy} & 0 \\ 0 & 0 & G_{zz} \end{bmatrix} \tag{2.60}$$

Noting that the operator $\nabla\nabla$ in the dyadic expression can be derived as

$$\nabla\nabla=\begin{bmatrix} \frac{d^2}{dx^2} & \frac{d^2}{dxdy} & \frac{d^2}{dxdz} \\ \frac{d^2}{dydx} & \frac{d^2}{dy^2} & \frac{d^2}{dydz} \\ \frac{d^2}{dzdx} & \frac{d^2}{dzdy} & \frac{d^2}{dz^2} \end{bmatrix} \tag{2.61}$$

therefore, the dyads can be expressed as follows

$$\begin{aligned} G_{xx} &= \sum_{m=0}^{\infty}\sum_{n=0}^{\infty}\frac{\epsilon_m\epsilon_n}{2abk_{mn}}\left(1+\frac{1}{k^2}\frac{d^2}{dx^2}\right)S_xS_x'C_yC_y'\;e^{-k_{mn}|z-z'|} \\ &= \sum_{m=0}^{\infty}\sum_{n=0}^{\infty}\frac{\epsilon_m\epsilon_n}{2abk_{mn}}\left(1-\frac{k_x^2}{k^2}\right)S_xS_x'C_yC_y'\;e^{-k_{mn}|z-z'|} \end{aligned} \tag{2.62}$$

$$\begin{aligned} G_{yy} &= \sum_{m=0}^{\infty}\sum_{n=0}^{\infty}\frac{\epsilon_m\epsilon_n}{2abk_{mn}}\left(1+\frac{1}{k^2}\frac{d^2}{dy^2}\right)C_xC_x'S_yS_y'\;e^{-k_{mn}|z-z'|} \\ &= \sum_{m=0}^{\infty}\sum_{n=0}^{\infty}\frac{\epsilon_m\epsilon_n}{2abk_{mn}}\left(1-\frac{k_y^2}{k^2}\right)C_xC_x'S_yS_y'\;e^{-k_{mn}|z-z'|} \end{aligned} \tag{2.63}$$

(2.64)

Table 2.1: Vector multiplication for all combination of slot part

Observed field	source	$\bar{u}$	$\bar{u}'$	$\bar{u} \cdot \overline{\overline{G}}_{int}(\bar{r}, \bar{r}') \cdot \bar{u}'$
bottom slot	bottom slot	$-\hat{x}$	$-\hat{x}$	G_{xx}
bottom slot	side slot	$-\hat{x}$	$\hat{y}\cos\theta + \hat{z}\sin\theta$	0
bottom slot	top slot	$-\hat{x}$	$\hat{x}$	$-G_{xx}$
side slot	bottom slot	$\hat{y}\cos\theta + \hat{z}\sin\theta$	$-\hat{x}$	0
side slot	side slot	$\hat{y}\cos\theta + \hat{z}\sin\theta$	$\hat{y}\cos\theta + \hat{z}\sin\theta$	$\cos\theta G_{yy}\cos\theta$ $+\sin\theta G_{zz}\sin\theta$
side slot	top slot	$\hat{y}\cos\theta + \hat{z}\sin\theta$	$\hat{x}$	0
top slot	bottom slot	$\hat{x}$	$-\hat{x}$	$-G_{xx}$
top slot	side slot	$\hat{x}$	$\hat{y}\cos\theta + \hat{z}\sin\theta$	0
top slot	top slot	$\hat{x}$	$\hat{x}$	G_{xx}

$$
\begin{aligned}
G_{zz} &= \sum_{m=0}^{\infty}\sum_{n=0}^{\infty} \frac{\epsilon_m \epsilon_n}{2abk_{mn}} \left(1 + \frac{1}{k^2}\frac{d^2}{dz^2}\right) C_x C_x' C_y C_y' \, e^{-k_{mn}|z-z'|} \\
&= \sum_{m=0}^{\infty}\sum_{n=0}^{\infty} \frac{\epsilon_m \epsilon_n}{2abk_{mn}} \left(1 + \frac{k_{mn}^2}{k^2}\right) C_x C_x' C_y C_y' \, e^{-k_{mn}|z-z'|}
\end{aligned} \tag{2.65}
$$

According to the expression of the internal Green's function, the vector multiplication on the (2.38) can be evaluated by evaluating the multiplication result for each variation of the slot part for observed and sources elements. As an example, both elements lie on the top wall. According to the direction vector $\bar{u} = \hat{x}$ and $\bar{u}' = \hat{x}$, the vector multiplication can be easily obtained.

$$
\bar{u} \cdot \overline{\overline{G}}_{int}(\bar{r}, \bar{r}') \cdot \bar{u}' = \begin{bmatrix} 1 \\ 0 \\ 0 \end{bmatrix}^T \begin{bmatrix} G_{xx} & 0 & 0 \\ 0 & G_{yy} & 0 \\ 0 & 0 & G_{zz} \end{bmatrix} \begin{bmatrix} 1 \\ 0 \\ 0 \end{bmatrix} = G_{xx} \tag{2.66}
$$

The result of the vector multiplication for all variations of the slot parts is listed in the table 2.1.

The table 2.1 shows the non zero results only contains of G_{xx}, except for both observed field and source are on the side slot part. Thus the explanation can be focused on the case of both elements on the top slot and on the side slot. While the other cases can be solved by taking analogous to the top slot case. Proceeding further, the component of the Green's function is substituted into the integral then it can be analyzed for each expression inside the double summation of the Green's

function. Firstly, the integral that both observed field and source lie on the top slot is evaluated.

$$
\begin{aligned}
Y_{ij}^{int} &= \iint_{S_i}\iint_{S_i} N_i(u)\cos\alpha G_{xx} N_j(u')\cos\alpha'\, ds'ds \\
&= \sum_{m=0}^{\infty}\sum_{n=0}^{\infty}\frac{\epsilon_m\epsilon_n}{2abk_{mn}}\left(1-\frac{k_x^2}{k^2}\right) \\
&\quad\cdot\iint_{S_i}\iint_{S_i} N_i(u)\cos\alpha S_x S_x' C_y C_y'\, e^{-k_{mn}|z-z'|} N_j(u')\cos\alpha'\, ds'ds \qquad (2.67)
\end{aligned}
$$

Considering the physical inner surface of the slot on the top wall, both surface integrals consist of the first integral over the x-axis and the second one over the z-axis. The range of first integration is the coordinate x of the first and second nodes of the surface element, noted as x_1 and x_2 for the observed field element and x_1' and x_2' for the source element. The second integral is taken over the slot width, from z_1 and $z_1 + w$. It is noting that the coordinate of both nodes is similar for the element on the top slot.

The solution of integral in (2.67) is explained by taking an example in case of $i = j = 1$. The integral is rearranged based on the domain of integration.

$$
\begin{aligned}
Y_{11}^{int} &= \sum_{m=0}^{\infty}\sum_{n=0}^{\infty}\frac{\epsilon_m\epsilon_n}{2abk_{mn}}\left(1-\frac{k_x^2}{k^2}\right)\cos(k_y y)\cos(k_y y') \\
&\quad\cdot\int_{x_1}^{x_2}\frac{x_2-x}{x_2-x_1}\cos\theta\sin(k_x x)dx\cdot\int_{x_1'}^{x_2'}\sin(k_x x')\frac{x_2'-x'}{x_2'-x_1'}\cos\theta dx' \\
&\quad\cdot\int_{z_1}^{z_1+w}\int_{z_1'}^{z_1'+w} e^{-k_{mn}|z-z'|}dz'dz \qquad (2.68)
\end{aligned}
$$

The first and second integral can be evaluated using the formula of partial integral, while the third can be alternately derived started from the inner integral over the z'.

$$
\begin{aligned}
\int_{z_1'}^{z_1'+w} e^{-k_{mn}|z-z'|}dz' &= \left[-\frac{e^{-k_{mn}|z-z'|}}{k_{mn}}\right]_{z_1'}^{z_1'+w} \qquad (2.69) \\
&= \frac{\left(1-e^{-k_{mn}w}\right)}{k_{mn}} e^{-k_{mn}|z-z_1'|} \qquad (2.70)
\end{aligned}
$$

Considering the integral of the exponential function yields the exponential function, the outer integral over z can be solved in the same way as over the z'.

Now, all integrals in (2.68) can be solved analytically and we get the analytical solution of Y_{11}. The other combination of other i and j can be derived using the same procedures as well.

$$
\begin{aligned}
Y_{11}^{int} = & \sum_{m=0}^{\infty}\sum_{n=0}^{\infty} \frac{\epsilon_m \epsilon_n}{2abk_{mn}} \left(1 - \frac{k_x^2}{k^2}\right) \cos(k_y y) \cos(k_y y') \\
& \cdot \cos\theta \left[-\frac{(x_2 - x)}{(x_2 - x_1)} \frac{\cos(k_x x)}{k_x} - \frac{1}{(x_2 - x_1)} \frac{\sin(k_x x)}{k_x^2} \right]_{x_1}^{x_2} \\
& \cdot \cos\theta \left[-\frac{(x_2' - x')}{(x_2' - x_1')} \frac{\cos(k_x x')}{k_x} - \frac{1}{(x_2' - x_1')} \frac{\sin(k_x x')}{k_x^2} \right]_{x_1'}^{x_2'} \\
& \cdot \left[\frac{(1 - e^{-k_{mn} w})^2}{k_{mn}^2} e^{-k_{mn}|z_1 - z_1'|} \right]
\end{aligned} \tag{2.71}
$$

$$
\begin{aligned}
Y_{12}^{int} = & \sum_{m=0}^{\infty}\sum_{n=0}^{\infty} \frac{\epsilon_m \epsilon_n}{2abk_{mn}} \left(1 - \frac{k_x^2}{k^2}\right) \cos(k_y y) \cos(k_y y') \\
& \cdot \cos\theta \left[-\frac{(x_2 - x)}{(x_2 - x_1)} \frac{\cos(k_x)}{k_x} - \frac{1}{(x_2 - x_1)} \frac{\sin(k_x x)}{k_x^2} \right]_{x_1}^{x_2} \\
& \cdot \cos\theta \left[-\frac{(x_2' - x')}{(x_2' - x_1')} \frac{\cos(k_x x')}{k_x} + \frac{1}{(x_2' - x_1')} \frac{\sin(k_x x')}{k_x^2} \right]_{x_1'}^{x_2'} \\
& \cdot \left[\frac{(1 - e^{-k_{mn} w})^2}{k_{mn}^2} e^{-k_{mn}|z_1 - z_1'|} \right]
\end{aligned} \tag{2.72}
$$

$$
\begin{aligned}
Y_{21}^{int} = & \sum_{m=0}^{\infty}\sum_{n=0}^{\infty} \frac{\epsilon_m \epsilon_n}{2abk_{mn}} \left(1 - \frac{k_x^2}{k^2}\right) \cos(k_y y) \cos(k_y y') \\
& \cdot \cos\theta \left[-\frac{(x_2 - x)}{(x_2 - x_1)} \frac{\cos(k_x x)}{k_x} + \frac{1}{(x_2 - x_1)} \frac{\sin(k_x x)}{k_x^2} \right]_{x_1}^{x_2} \\
& \cdot \cos\theta \left[-\frac{(x_2' - x')}{(x_2' - x_1')} \frac{\cos(k_x x')}{k_x} - \frac{1}{(x_2' - x_1')} \frac{\sin(k_x x')}{k_x^2} \right]_{x_1'}^{x_2'} \\
& \cdot \left[\frac{(1 - e^{-k_{mn} w})^2}{k_{mn}^2} e^{-k_{mn}|z_1 - z_1'|} \right]
\end{aligned} \tag{2.73}
$$

$$
\begin{aligned}
Y_{22}^{int} = & \sum_{m=0}^{\infty}\sum_{n=0}^{\infty} \frac{\epsilon_m \epsilon_n}{2abk_{mn}} \left(1 - \frac{k_x^2}{k^2}\right) \cos(k_y y) \cos(k_y y') \\
& \cdot \cos\theta \left[-\frac{(x_2 - x)}{(x_2 - x_1)} \frac{\cos(k_x x)}{k_x} + \frac{1}{(x_2 - x_1)} \frac{\sin(k_x x)}{k_x^2} \right]_{x_1}^{x_2} \\
& \cdot \cos\theta \left[-\frac{(x_2' - x')}{(x_2' - x_1')} \frac{\cos(k_x x')}{k_x} + \frac{1}{(x_2' - x_1')} \frac{\sin(k_x x')}{k_x^2} \right]_{x_1'}^{x_2'} \\
& \cdot \left[\frac{(1 - e^{-k_{mn} w})^2}{k_{mn}^2} e^{-k_{mn}|z_1 - z_1'|} \right]
\end{aligned} \tag{2.74}
$$

The second case, both observed field and source are on the narrow- wall slot. Taking the result of the vector multiplication on the table 2.1, the expression of the Y_{ij}^{int} is obtained as follow

$$
\begin{aligned}
Y_{ij}^{int} &= \iint_{S_i}\iint_{S_i} N_i(u)\left[\cos\theta G_{yy}\cos\theta + \sin\theta G_{zz}\sin\theta\right] N_j(u')\, ds'ds \qquad (2.75)\\
&= \sum_{m=0}^{\infty}\sum_{n=0}^{\infty}\frac{\epsilon_m\epsilon_n}{2abk_{mn}}\\
&\left[\left(1-\frac{k_y^2}{k^2}\right)\iint_{S_i}\iint_{S_i} N_i(u)\cos\theta C_x C_x' S_y S_y'\, e^{-k_{mn}|z-z'|}\cos\theta N_j(u')\, ds'ds\right.\\
&\left.+\left(1+\frac{k_{mn}^2}{k^2}\right)\iint_{S_i}\iint_{S_i} N_i(u)\sin\theta C_x C_x' C_y C_y'\, e^{-k_{mn}|z-z'|}\sin\theta N_j(u')\, ds'ds\right]
\end{aligned}
$$

The integrals of G_{yy} and G_{zz} are derived separately, but using the same procedures. The four integrals are over the area of observed field element (u and z) and source element(u and z') ' that can be successively derived from the inner to outer one. The integrals over z and z' has solution as derived in (2.70). While the u and u' are evaluated by considering that $y = u\cos\theta$,$y' = u'\cos\theta$,$z = u\sin\theta$ and $z' = u'\sin\theta$. The integrals becomes in the form of $N_i \sin(k_y u\cos\theta)e^{(k_{mn}u\sin\theta)}$ and $N_i\cos(k_y u\cos\theta)e^{(k_{mn}u\sin\theta)}$ that can be derived using the formulas of the partial integral and the integral of the exponential and trigonometric function taken from [22] as follows

$$\int e^{\alpha t}\sin\beta t\, dt = \frac{e^{\alpha t}}{\alpha^2+\beta^2}(\alpha\sin\beta t - \beta\cos\beta t) + c \qquad (2.76)$$

$$\int e^{\alpha t}\cos\beta t\, dt = \frac{e^{\alpha t}}{\alpha^2+\beta^2}(\alpha\cos\beta t + \beta\sin\beta t) + c \qquad (2.77)$$

Finally, the expression of Y_{ij} of the second case is obtained. The final expression for $i = j = 1$ is shown in (2.78) below, while the others variation of i and j can be obtained by using the same procedures.

$$
\begin{aligned}
Y_{ij}^{int} &= \sum_{m=0}^{\infty}\sum_{n=0}^{\infty}\frac{\epsilon_m\epsilon_n}{2abk_{mn}}\frac{(1-e^{-k_{mn}w})^2}{k_{mn}^2}\\
&\cdot\left\{\left(1-\frac{k_y^2}{k^2}\right)\left[A_i(u)\left[A_j(u')e^{-k_{mn}\sin\theta|u-u'|}\right]_{u_1}^{u_2}\right]_{u_1'}^{u_2'}\right.\\
&\left.+\left(1+\frac{k_{mn}^2}{k^2}\right)\left[B_i(u)\left[B_j(u')e^{-k_{mn}\sin\theta|u-u'|}\right]_{u_1}^{u_2}\right]_{u_1'}^{u_2'}\right\} \qquad (2.78)
\end{aligned}
$$

with

$$
\begin{aligned}
A_1(u) &= \frac{(u_2-u)}{(u_2-u_1)}\frac{1}{(\alpha^2+\beta^2)}(\alpha\sin(\beta u)-\beta\cos(\beta u)) \\
&+\frac{1}{(u_2-u_1)}\frac{\alpha}{(\alpha^2+\beta^2)^2}(\alpha\sin(\beta u)-\beta\cos(\beta u)) \\
&-\frac{1}{(u_2-u_1)}\frac{\beta}{(\alpha^2+\beta^2)^2}(\alpha\cos(\beta u)+\beta\sin(\beta u)) \qquad (2.79)\\
A_2(u) &= \frac{(u-u_1)}{(u_2-u_1)}\frac{1}{(\alpha^2+\beta^2)}(\alpha\sin(\beta u)-\beta\cos(\beta u)) \\
&-\frac{1}{(u_2-u_1)}\frac{\alpha}{(\alpha^2+\beta^2)^2}(\alpha\sin(\beta u)-\beta\cos(\beta u)) \\
&+\frac{1}{(u_2-u_1)}\frac{\beta}{(\alpha^2+\beta^2)^2}(\alpha\cos(\beta u)+\beta\sin(\beta u)) \qquad (2.80)\\
B_1(u) &= \frac{(u_2-u)}{(u_2-u_1)}\frac{1}{(\alpha^2+\beta^2)}(\alpha\cos(\beta u)+\beta\sin(\beta u)) \\
&+\frac{1}{(u_2-u_1)}\frac{\alpha}{(\alpha^2+\beta^2)^2}(\alpha\cos(\beta u)+\beta\sin(\beta u)) \\
&+\frac{1}{(u_2-u_1)}\frac{\beta}{(\alpha^2+\beta^2)^2}(z_y\sin(\beta u)+\beta\cos(\beta u)) \qquad (2.81)
\end{aligned}
$$

$$
\begin{aligned}
B_1(u) &= \frac{(u-u_1)}{(u_2-u_1)}\frac{1}{(\alpha^2+\beta^2)}(\alpha\cos(\beta u)+\beta\sin(\beta u)) \\
&-\frac{1}{(u_2-u_1)}\frac{\alpha}{(\alpha^2+\beta^2)^2}(\alpha\cos(\beta u)+\beta\sin(\beta u)) \\
&-\frac{1}{(u_2-u_1)}\frac{\beta}{(\alpha^2+\beta^2)^2}(z_y\sin(\beta u)+\beta\cos(\beta u)) \qquad (2.82)
\end{aligned}
$$

where

$$\alpha = -k_{mn}\sin\theta \qquad (2.83)$$

$$\beta = k_y\cos\theta \qquad (2.84)$$

Hence, the expressions are on the form that are ready for writing into computer program. The required order of the summations (m, n) is investigated and the result is shown in Fig. 2.7. The graph shows that it need about 200 iteration both m and n to obtain an acceptable result.

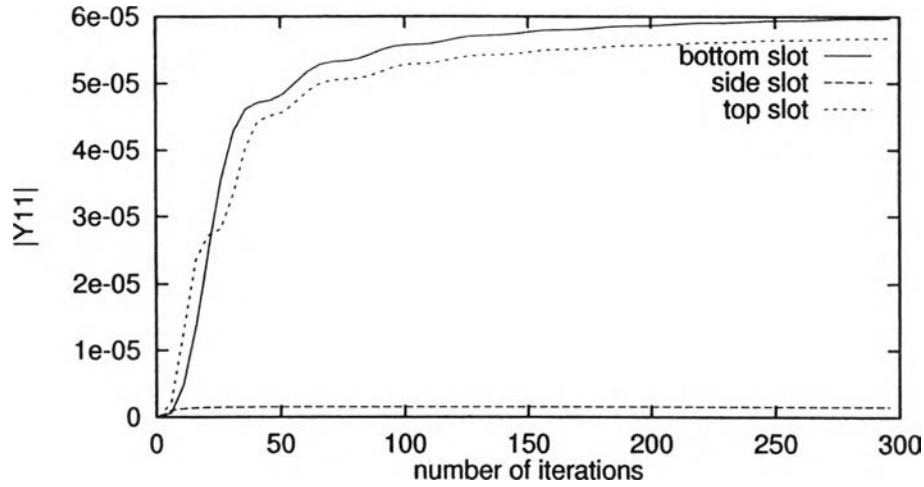

Figure 2.7: Convergent value of integral calculation on the internal surface.

2.3.5 The formulation of fields on the outer surfaces

The field on the outer or scattering surface is shown on the third integral of (2.22). It has the same form as the integral on the inner surface but it uses a different kind of Green's function . The initial procedure to derive is similar to the inner surface and we get the formulation in terms of integral over the external surface element.

$$\iint_{S_e}\iint_{S_e} \phi(\bar{r})\cos\alpha\ \bar{u}\cdot\bar{\bar{G}}_{ext}(\bar{r},\bar{r}')\cdot\bar{u}'\ \phi(\bar{r})\cos\alpha'\ ds'ds$$
$$= \sum_{e_{ext}}\sum_{e'_{ext}}\left[\sum_{i=1}^{2}\sum_{j=1}^{2}\phi_i Y_{ij}^{ext}\phi_j\right] \tag{2.85}$$

where e_{ext} is the element on the outer surface and coefficient of $Y_{ij}^{(ext)}$ is given by

$$Y_{ij}^{ext} = \iint_{S_i}\iint_{S_i} N_i(u)\cos\alpha\ \bar{u}\cdot\bar{\bar{G}}_{ext}(\bar{r},\bar{r}')\cdot\bar{u}'\ N_j(u')\cos\alpha'\ ds'ds \tag{2.86}$$

with i and j are the local nodes of the surface element.

The external Green's function uses the 90° wedge Green's function that has been introduced in [8]. This special Green's function is derived to take into account the scattering effect of a single corner around the field and the source regions. The detail formulation is conducted in the next subsection.

2.3.5.1 The formulation of 90° wedge Green's function

In order to account the effect of the waveguide corners in the edge slot analysis, Jan *et al.* introduced the 90° wedge Green's function [8]. They derived from the dyadic Green's function for a perfectly conducting wedge that formulated in [19] chapter 9 . It has been derived in [8] specified for 90° wedge. The formulation is rearranged in more compactly form as follows

$$\begin{aligned}\overline{\overline{G}}(\bar{r},\bar{r}') &= -\frac{j}{6\pi}\sum_{n=0}^{\infty}(2-\delta_0)(\pm 1)^n \cdot \\ &\left[\hat{r}\hat{r}(g_{v-1}+g_{v+1})/2+\hat{z}\hat{z}g_v-\frac{1}{k^2}\nabla_t\nabla_t' g_v\right]_{v=2/3n} \qquad (2.87)\end{aligned}$$

where k is the free space wave-number, δ_0 is unity as $v = 0$ while zero for other v's. The ± 1 means that it is equal to +1 when $\bar{r}$ and $\bar{r}'$ lie on the same side of the wedge, while equal to $(-1)^n$ when $\bar{r}$ and $\bar{r}'$ lie on the different sides of the wedge. The functions $g_\mu(\mu = v-1, v, \text{ or } v+1)$ are defined by

$$g_\mu(r,r',z,z') = 2\int_0^\infty J_\mu(\eta r_m)H_\mu(\eta r_M)\cos h|z-z'|dh \qquad (2.88)$$

$$r_m = \min(r,r'), \quad r_M = \max(r,r') \qquad (2.89)$$

η is related to the h by $\eta^2 = k^2 - h^2$. J_μ and $H^{(2)_\mu}$ are the Bessel function and the Hankel function of second kind respectively. The coordinates system has to be adapted in the calculation with relation as an example on Fig. 2.8. Simplifying the expression of the g_μ, Jan *et al.* has rewritten it in normalized form as

$$\begin{aligned}g_\mu(\tilde{r}_m,\tilde{r}_M,\tilde{z}_d) &= 2k\int_0^\infty J_\mu(-j\sqrt{\zeta^2-1}\tilde{r}_m) \\ &\quad \cdot H_\mu(-j\sqrt{\zeta^2-1}\tilde{r}_M)\cos(h\tilde{z}_d)d\zeta \qquad (2.90)\end{aligned}$$

$$\zeta = \frac{h}{k} \qquad (2.91)$$

$$\frac{\tilde{r}_m}{r_m} = \frac{\tilde{r}_M}{r_M} = \frac{\tilde{z}_d}{z_d} = k \qquad (2.92)$$

$$z_d = |z-z'| \qquad (2.93)$$

The application of this external Green's function can be explained by considering the source and field points which is shown by four case in Fig. 2.5. In the case

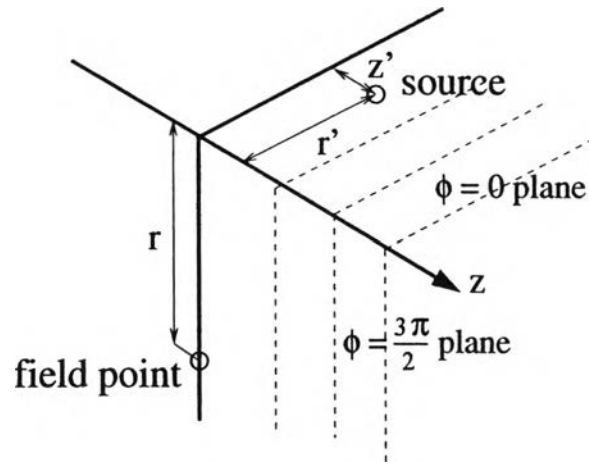

Figure 2.8: Modeling the field caused by magnetic current on the external surfaces of slot.

of one lies in the broad wall, while the other lies in the side wall as shown in Fig. 2.9.a, the field from source to the field point is scattered by the between corner is derived using those 90° wedge Green's Functions. The scattering field from other corner is neglected.

Fig. 2.9.b, both points lie in on the broad wall. In this case, although the conventional half space Green's function may serve as a crude approximation, but the wedge Green's function should have better result, especially when both points are close to the waveguide corner.

In case of Fig. 2.9.c, both points lie on the side wall, therefore the scattering effect from both corner must be considered, The Green's function is evaluated by the summation of the wedge Green's function from two corners minus the half space Green's function.

In case of Fig. 2.9.d, one point lies on bottom wall and the other is on top wall of waveguide. The contribution is now due to the consecutive scattering from the two corners. It is neglected in the calculation.

The half space Green's function used in couple with the wedge Green's function in case of Fig. 2.9.b is expressed as

$$\overline{\overline{G}}(\bar{r},\bar{r}') = (k^2 + \nabla\nabla)\frac{e^{-jk\bar{r}}}{2\pi\bar{r}} \tag{2.94}$$

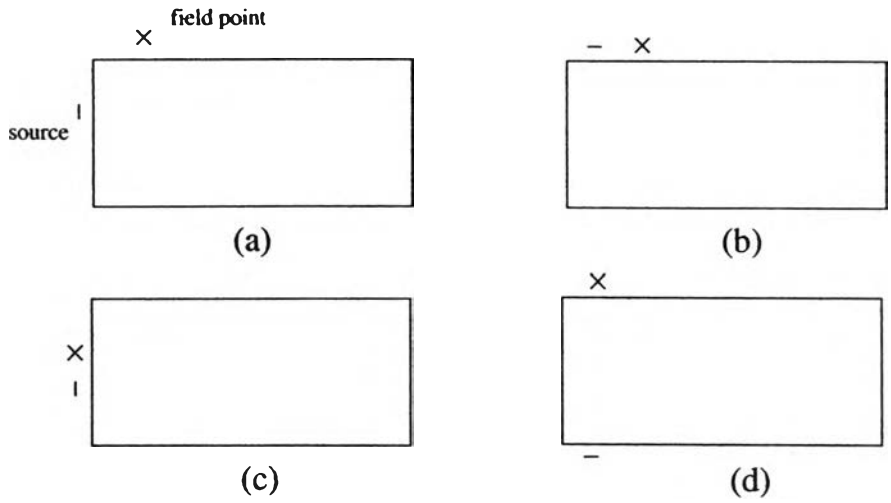

Figure 2.9: Example of source and field point in the coordinates system used in wedge Green's function calculation.

where $\bar{r} = \sqrt{(x-x')^2 + (y-y') + (z-z')}$ is the distance between the source and the observed field points.

2.3.5.2 The solution of integral on the external surface

The shape domain of the integral in (2.86) is similar to the integral on the internal surface that contains the internal Green's function. The domain can be decomposed into u, z, u' and z'. The first two parameters are the area of the observed field element and the rests are the source element.

$$Y_{ij}^{ext} = \int_{u_1}^{u_2}\int_{z}^{z+w} \int_{u_1'}^{u_2'}\int_{z'}^{z'+w} N_i(u)\cos\alpha\ \bar{u}\cdot\overline{\overline{G}}_{ext}(\bar{r},\bar{r}')\cdot\bar{u}'\ N_j(u')\cos\alpha'\ dz'du'dz\ du \tag{2.95}$$

The vector multiplication inside the integration is evaluated in the same way as in the internal surface and considering the transformation of the rectangular coordinates system to the cylindrical one as used in the calculation of the external Green's function. The result of this operation is listed on Table 2.2.

The complicated form of the external Green's function causes the integral in (2.95) can not be solved analytically, thus it is calculated using the Gauss quadrature integral approximations. Since the shape of the area of the element on the side slot is inclined, it is more convenient to solve by four successive line integral

Table 2.2: Vector multiplications for all combination of slot part

Observed field	source	$\bar{r}$	$\bar{r}$'	$\bar{u} \cdot \overline{\overline{G}}_{int}(\bar{r}, \bar{r}') \cdot \bar{u}'$
bottom slot	bottom slot	$\hat{x}$	$\hat{x}$	G_{rr}
bottom slot	side slot	$\hat{x}$	$\hat{y}$	$G_{rr}\cos\theta$
bottom slot	top slot	$\hat{x}$	$\hat{x}$	neglected
side slot	bottom slot	$\hat{y}$	$\hat{x}$	$G_{rr}\cos\theta$
side slot	side slot	$\hat{y}$	$\hat{y}$	$\cos\theta G_{rr}\cos\theta$
				$+\sin\theta G_{zz}\sin\theta$
side slot	top slot	$\hat{y}$	$\hat{x}$	$G_{rr}\cos\theta$
top slot	bottom slot	$\hat{x}$	$\hat{x}$	neglected
top slot	side slot	$\hat{x}$	$\hat{y}$	$G_{rr}\cos\theta$
top slot	top slot	$\hat{x}$	$\hat{x}$	G_{rr}

approximations rather than two area integral to simplify the programming.

2.3.6 Matrix Assembly and Finalization

Based on the finite element procedures, the matrix forms of the fields in the cavity and both boundary surfaces are assembled into a global matrix using the relation of the variational equation in (2.22).

$$\begin{aligned}
\psi' &= \frac{1}{2}\sum_{e}\left[\sum_{i=1}^{3}\sum_{j=1}^{3}\phi_i G_{ij}^{(e)}\phi_j\right] \\
&\quad +\frac{1}{2}\sum_{e_{int}=1}^{N}\sum_{e'_{int}=1}^{N}\left[\sum_{i=1}^{2}\phi_i^{(e_{int})}Y_{ij}^{(e_{int})}\phi_j^{(e_{int})}\right] \\
&\quad +\frac{1}{2}\sum_{e_{ext}=1}^{N}\sum_{e'_{ext}=1}^{N}\left[\sum_{i=1}^{2}\phi_i^{(e_{ext})}Y_{ij}^{(e_{ext})}\phi_j^{(e_{ext})}\right] \\
&\quad -\sum_{i=1}^{2}H_i^{(e_{int})}\phi_i^{(e_{int})} \\
&= \frac{1}{2}[\phi]^T[F][\phi] - [\phi]^T[h^{inc}] \qquad (2.96)
\end{aligned}$$

where $[\phi]$ is a vector consisting of the unknowns of all nodes and the superscript T denotes the vector transpose.

Proceeding further, the stationary condition of the variational equation is determined by taking the first derivative of (2.96) and considering the boundary condition where the electric field on both ends of slot must be vanished. The expression becomes

$$[F][\phi] = [h^{inc}] \tag{2.97}$$

Finally, the last step of the finite element method is solving the linear equation in (2.97) that can be done by applying the Gaussian Elimination method.

Accomplishing the finite element method, the electric field distribution along the slot can be determined and it can be used to calculate the equivalent network parameter such as the reflection coefficient and the normalized admittance and other parameter such radiation pattern, resonant length, etc.

2.4 Admittance properties of edge slot

This section explains how to calculate the network equivalent or the admittance properties of an edge slot from the electric field distribution obtained in the analysis of the combined finite element and moment methods.

Initially, the reflection coefficient Γ is calculated from the electric field distribution along the slot with the relation recalled from (2.7) as follows.

$$\Gamma = \frac{(\pi/a)^2}{\omega\mu_0\beta_{inc}ab}\int_{slot} \overline{E}_s \times \overline{H}^{+}_{inc} \cdot \bar{n}\, ds \tag{2.98}$$

where $\overline{H}^{+}_{inc}$ is the forward propagating magnetic field of the TE_{10} mode, $\bar{n}$ is the unit vector inward normal to the waveguide wall and $\overline{E}_s$ is the electric field along the slot that has direction across the slot width.

$$\overline{E}_s = \hat{v}\phi = -\hat{y}\phi\sin\theta + \hat{z}\phi\cos\theta \tag{2.99}$$

From the result of the analysis, the electric field is known on each node, while on the other points is calculated by linear interpolation of two closest nodes.

According to the structure of edge slot that has parts on the bottom, narrow

and top walls, the $\bar{n}$ has different direction on each part.

$$\begin{array}{ll} \bar{n} = \hat{y} & \text{slot on the bottom wall} \\ \bar{n} = \hat{x} & \text{slot on the side wall} \\ \bar{n} = -\hat{y} & \text{slot on the top wall} \end{array} \tag{2.100}$$

The integrand of (2.98) can be evaluated for each slot part by the below relation

$$\begin{aligned} (\overline{E}_s \times \overline{H}_{inc}) \cdot \bar{n} &= \bar{n} \cdot (\overline{E}_s \times \overline{H}_{inc}) \\ &= \begin{vmatrix} n_x & n_y & n_z \\ 0 & -\phi \sin\theta & \phi \cos\theta \\ H_x^{inc} & 0 & H_z^{inc} \end{vmatrix} \end{aligned} \tag{2.101}$$

and we get

$$\begin{array}{ll} (\overline{E}_s \times \overline{H}_{inc}) \cdot \bar{n} = \phi \ \cos\theta \ H_x^{inc} & \text{slot on the bottom wall} \\ (\overline{E}_s \times \overline{H}_{inc}) \cdot \bar{n} = -\phi \ \sin\theta \ H_z^{inc} & \text{slot on the bottom wall} \\ (\overline{E}_s \times \overline{H}_{inc}) \cdot \bar{n} = -\phi \ \cos\theta \ H_x^{inc} & \text{slot on the top wall} \end{array} \tag{2.102}$$

Now, the reflection coefficient can be calculated easily by a summation of the integral on each element. Finally, the admittance parameters can be calculated using (2.6) and get the equivalent conductance and susceptance of the slot.

2.5 Radiation pattern of edge slot

The radiation patterns of the edge slot antenna are rarely reported in the literature because the patterns are not easily obtained since the Green's function for the specific structure of edge slot is not available.

This research tries to predict the radiation pattern of the edge slot by assuming the wrapped parts as the extension of the narrow part on the infinite conductor plane and applying a common half space Green's function. The coordinate system is transformed to ease the formulation of the calculation as depicted in Fig. 2.10.

The radiation pattern can be evaluated using the formulation of the far field pattern for a rectangular aperture [23].

$$\overline{E}(\bar{r}) = \frac{ik\cos\vartheta}{2\pi r} e^{-ikr} \bar{f}(k\sin\vartheta\cos\varphi, k\sin\vartheta\sin\varphi) \tag{2.103}$$

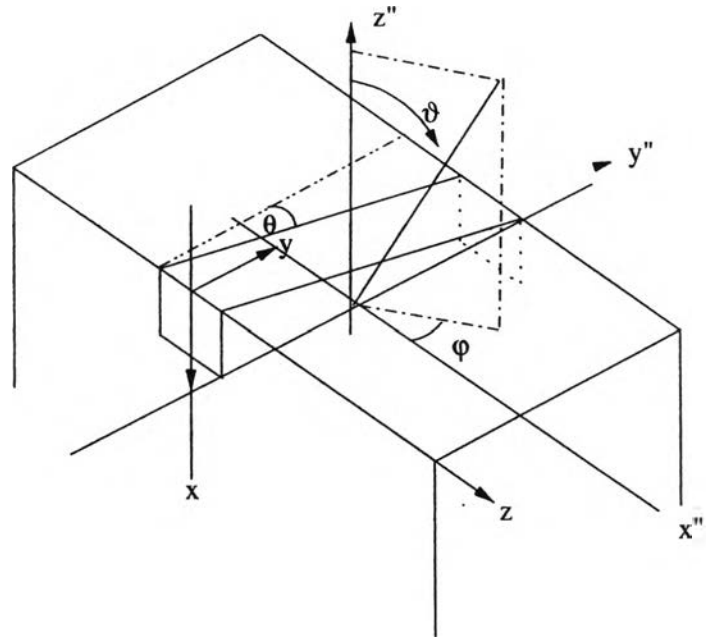

Figure 2.10: Coordinate transformation for the calculation of radiation patterns

where

$$\begin{aligned} \bar{f}(k_x, k_y) &= \int_{slot} \overline{E}_s(x", y") e^{-ik_x x" - ik_y y"} dx" dy" \qquad (2.104) \\ k_x &= k \sin\vartheta \cos\varphi \\ k_y &= k \sin\vartheta \sin\varphi \end{aligned}$$

The $\overline{E}_s = \hat{x}"\phi$ is taken from the result of the analysis that has direction across the slot. The integral is calculated for each element by the similar way as for the calculation of the admittance properties.